Femtosecond Terahertz Radiation from Femtoslicing at BESSY

K. Holldack,[1,*] S. Khan,[1] R. Mitzner,[2] and T. Quast[1]

[1]*Berliner Elektronenspeicherring-Gesellschaft für Synchrotronstrahlung m.b.H. (BESSY), Albert-Einstein-Straße 15, 12489 Berlin, Germany*

[2]*Physikalisches Institut der Universität Münster, Wilhelm-Klemm-Strasse 10, 48149 Münster, Germany*

(Received 1 December 2005; published 8 February 2006)

Femtosecond far-infrared radiation pulses in the THz spectral range were observed as a consequence of the energy modulation of 1.7 GeV electrons by femtosecond laser pulses in the BESSY storage ring in order to generate femtosecond x-ray pulses (''femtoslicing''). In addition to being crucial for diagnostics of the laser-electron interaction, the THz radiation itself is useful for experiments where intense ultrashort THz pulses of well-defined temporal and spectral characteristics are required.

DOI: 10.1103/PhysRevLett.96.054801 PACS numbers: 41.75.Ht, 41.60.Cr, 42.65.Re

Femtosecond (fs) x-ray pulses as well as THz radiation are currently of particular interest in ultrafast optical science [1,2]. The ability to generate time synchronized x-ray and THz pulses is of interest for many experiments. With free-electron lasers (FELs) not yet being available in the photon energy range between 100 eV and several keV, there are few ongoing projects to generate fs x-ray pulses in third generation synchrotron radiation sources via ''femtoslicing,'' which was proposed [3] and experimentally demonstrated at the Advanced Light Source (ALS) in Berkeley [4] with radiation from a bend magnet, while the first undulator-based facility was constructed and successfully commissioned at BESSY [5]. Here, electrons with a kinetic energy of 1.7 GeV copropagate with a fs laser pulse in a planar undulator (U139 with 10 periods of 139 mm length), the ''modulator,'' where the electron energy is modulated with the periodicity of the laser wavelength. These off-energy electrons are transversely displaced by a bend magnet in order to extract their radiation in a subsequent elliptical undulator (UE56 with 30 periods of 56 mm length), the ''radiator.'' A detailed description of the layout and angular separation scheme employed at BESSY was given in [6]. The laser pulses with a pulse energy of ≤ 2.8 mJ and 30–50 fs [full width at half maximum (FWHM)] at a repetition rate of 1 kHz are produced by a Ti:sapphire laser-system, using chirped-pulse amplification (CPA) [7]. Figure 1 shows the result of a tracking calculation demonstrating the evolution of the electron density in the magnetic lattice following the modulator. The emission of coherent synchrotron radiation (CSR) in the infrared range was predicted [4] to occur as a consequence of a longitudinal density modulation on a sub-mm length scale. Proof-of-principle results of laser-induced CSR in the femtoslicing process were recently reported from the ALS showing narrow band spectra observed using a bolometer that integrates over 0.7 ms [8]. At BESSY, first laser-induced CSR pulses were found with a fast detector of 0.3 μs risetime [9].

This Letter reports the first observation of broadband THz CSR at a beam line directly following the energy modulation of electrons by fs laser pulses, its spectral characterization, and time-domain reconstruction. These pulses are naturally synchronized to fs x-ray pulses. Besides being crucial for setting up and optimizing femtoslicing experiments, the laser-induced THz radiation itself is a useful source for time-resolved experiments. The temporal decay of the THz power over several storage ring turns will be described and the need to carefully discriminate first-turn radiation from successive emission in order to obtain fs THz pulses will be demonstrated. A new method to optimize the laser-electron interaction is introduced.

As shown in Fig. 1, THz radition is extracted at a bend magnet 11 m downstream of the modulator, the closest position at which the installation of a specialized beam line with an acceptance of 60 mrad horizontally and 15 mrad vertically was possible. Here, a longitudinal electron density modulation on the scale of 0.1 mm gives rise to CSR in the THz range [10]. In the present case the coherent spectral power density at radiation frequencies ω can be estimated by

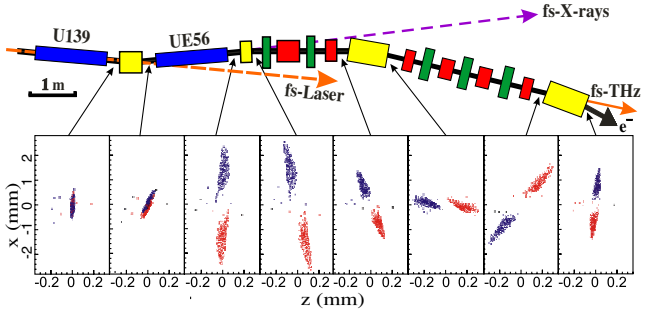

FIG. 1 (color online). Top view of BESSY II storage ring magnets downstream of the femtoslicing modulator (U139) and radiator (UE56), and horizontal-longitudinal (x-z) projection of electrons with a laser-induced energy modulation $\Delta E/E > 0.3\%$.

$$P_{\mathrm{coh}}(\omega) \sim \left(N_0 \frac{\sigma_L}{\sigma_0}\right)^2 p(\omega)|F(\omega)|^2. \quad (1)$$

Here, σ_L is the laser pulse length, N_0 is the number of electrons in the bunch, σ_0 is the bunch length, $p(\omega)$ is the incoherent power emitted by a single electron and $|F(\omega)|$ the magnitude of the Fourier transform of the longitudinal electron density. Assuming that all displaced electrons would emit coherently at equal phases using $\sigma_0 = 15$ ps, $\sigma_L = 15$ fs, and $N_0 = 10^{10}$, then P_{coh} would exceed the incoherent spectral power density $P_{\mathrm{inc}} = N_0 p(\omega)$ by a factor of 10^4. Despite the fact that the transmission functions of the beamline and the detectors as well as the cutoff function of the storage ring vacuum vessel [11] reduce this ratio, the coherent power from femtoslicing of a single bunch of 10^{10} electrons can still exceed the incoherent power of 400 bunches in the storage ring.

THz radiation was detected using liquid He-cooled bolometers [12] and even with detectors operated at room temperature [13]. At a laser pulse energy of 2.1 mJ and a bunch charge of 4.8 nC, a THz pulse energy of 4.5 nJ was observed. Assuming a pulse length of ~300 fs (FWHM) as determined below, the peak power density amounts to 15 kW/mm^2 being comparable to that of laser-based sources in the same spectral range [14]. An oscilloscope trace recorded from an InSb bolometer is shown in the inset of Fig. 2, where femtoslicing was performed at BESSY during user operation at a multibunch current of 220 mA in 350 bunches leaving a gap of 100 ns. The laser interacted with an additional bunch of 4 mA ($N_0 = 2 \times 10^{10}$) in the gap. A typical shot-to-shot stability of the THz signal of 5% is observed. The spectrally integrated THz signal of an InSb bolometer is routinely used to optimize the laser-electron interaction in the U139 modulator with respect to transverse, temporal, and spectral overlap. At a bunch current above 4.5 mA additional sub-THz CSR—quasi-periodic spontaneous bursting as well as bursts locked to the laser repetition rate—is observed [9]. This background is suppressed by tuning a lock-in amplifier to a higher harmonic of the laser repetition rate, or by using a 10 cm^{-1} high-pass filter. A THz signal with a time resolution limited by the detector rise time of 0.3 μs is plotted in Fig. 2 over 16 turns in the storage ring, corresponding to one of the peaks shown in the inset. The "afterglow" of THz radiation indicates that the laser-induced density modulation persists over many turns. Radiation from the first turn is detected with reduced efficiency since the spectral response of the InSb detector rapidly decreases above 33 cm^{-1} (1 THz) favoring long-wavelength radiation from later turns. Numerical tracking calculations including the full magnetic lattice were started but their discussion is beyond the scope of this Letter. A simple explanation based on momentum-compaction arguments will be given below. Spectral measurements of signals gated on individual turns as shown in Fig. 3 demonstrate that only mm waves are emitted after the first turn corresponding to a ps modulation of the electron density. The data confirm earlier observations that pulses from later turns can be removed by filters [15].

The temporal laser pulse parameters were varied by changing the grating separation in the stretcher of the laser system, introducing a longitudinal chirp (i.e., a variation of frequency with time) to the laser pulse. The pulse length ranging from 45 fs for the unchirped pulse to about 500 fs was derived from an autocorrelator measurement. Figure 4 illustrates the influence of the grating separation on the THz signal. At 75 fs pulse length, signals from later turns are significantly suppressed. The largest ratio of 1st-to-2nd turn THz intensity indicates a maximum energy modulation. This deviates from the minimum-chirp condition due to positive group-velocity dispersion caused by lenses and the vacuum port in the laser beam path. Maximum energy modulation at this grating position was confirmed by two independent measurements (i) observing the bunch lifetime while probing the transverse distribution of energy-modulated electrons with a scraper, and (ii) measuring the

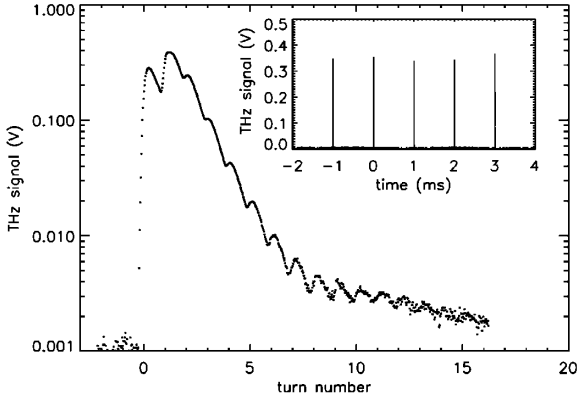

FIG. 2. THz radiation signal as measured using an InSb detector operated at 4.2 K as a function of time plotted over 16 storage ring turns (12.8 μs, 1turn = 800 ns) and a single trace over 6 ms (inset).

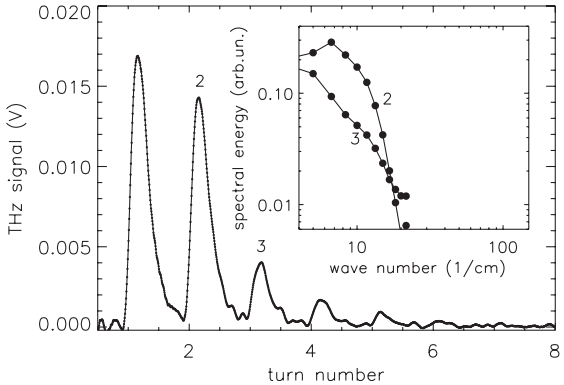

FIG. 3. THz radiation signal as measured over 8 storage ring turns using an InSb detector operated at 10 K and spectra from the 2nd and 3rd turn, respectively. The full spectrum from the first turn is not accessible by this detector type.

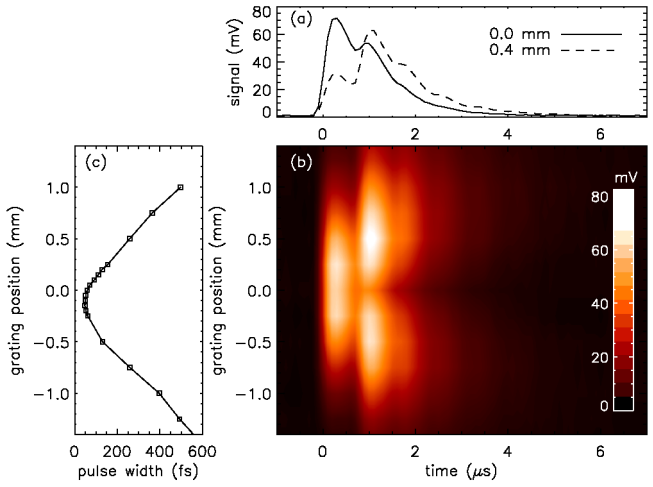

FIG. 4 (color online). THz signal versus time over 6 μs (1 turn = 800 ns) for two different positions of the stretcher grating in the CPA amplifier (a). The full set of these traces for a large number of grating positions was plotted color coded in (b), while the corresponding variation in laser pulse width (FWHM) was measured with an autocorrelator (c). Note that the emitted THz power can be shifted from the 1st turn to the 2nd turn for large laser pulse widths.

angular distribution of soft x-rays in the range of 600–900 eV produced by these electrons [5].

The decay of the THz signal shown in Fig. 2 is due the nonisochronicity of the storage ring. The average path length differences ΔL along the magnetic lattice for the energy-modulated electrons increase about a factor of 10 faster than for the electrons having only the natural energy spread. To first order (neglecting betatron oscillations), the path length varies according to $\Delta L = nL_0\alpha\Delta p/p$ [16], where $\Delta p/p \sim \Delta E/E$ is the momentum deviation of the electrons, $\alpha = 7.5 \times 10^{-4}$ is the momentum-compaction factor, $L_0 = 240$ m is the ring circumference, and n is the number of turns. For $\Delta E/E$ close to 1% as required for the purpose of fs x-ray pulse generation, radiation from successive turns is already significantly suppressed by the cutoff of the beam line at $\sim$4 cm^{-1} ($\Delta L \sim 2.5$ mm). Thus, optimizing the energy modulation helps to suppress a ps background from later turns for fs THz spectroscopy. The same result can be obtained by increasing the momentum-compaction factor which controls the persistence of the density modulation.

For the temporal and spectral characterization [17] of the first-turn THz pulses a slow (0.2 ms fall time) Si bolometer at 4.2 K suitable for broadband spectral measurements was employed together with a 600 cm^{-1} (18 THz) low-pass filter, a 10 cm^{-1} high-pass filter (suppressing later turns), and a Martin-Puplett spectrometer [18]. Results of time-domain autocorrelation measurements from this setup are compared in Fig. 5 for CSR from a Gaussian bunch of 0.15 μA and 1.2 ps length (rms), when the storage ring was operated with a reduced

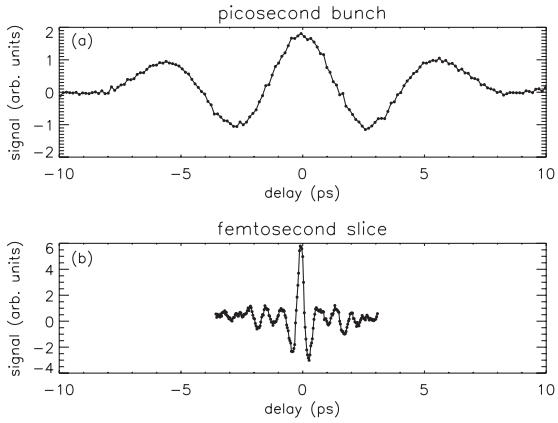

FIG. 5. Far-infrared interferograms of THz radiation (a) from an electron bunch of 1.2 ps (rms) length, produced by lowering the momentum-compaction factor and (b) from a longitudinal density modulation induced by the fs laser pulses.

momentum-compaction factor [19], and THz radiation from femtoslicing at 2 mA bunch current. The center peak of the lower interferogram shows a FWHM of 230 fs, corresponding to 70 μm path length difference in the interferometer, which clearly indicates the fs nature of the THz pulses. According to [17], this would correspond to a THz emission from a fs Gaussian bunch of $\sigma_z = 138$ fs. However, the density modulation is expected to be non-Gaussian, which is confirmed by the corresponding spectrum shown in Fig. 6. Its characteristic shape demonstrates the broadband nature and the peaked spectral distribution of laser-induced radiation compared to CSR emission from a ps Gaussian bunch. Effects of beam line transmission are corrected by measuring the incoherent spectra from regular multibunch operation in the storage ring. In order to reconstruct the electron density modulation $\rho(z)$ from the spectra, the pulse shape in the time domain was assumed to consist of two Gaussians, $G_1(z, \sigma_1)$ and $G_2(z, \sigma_2)$ where σ_1 corresponds to the dis-

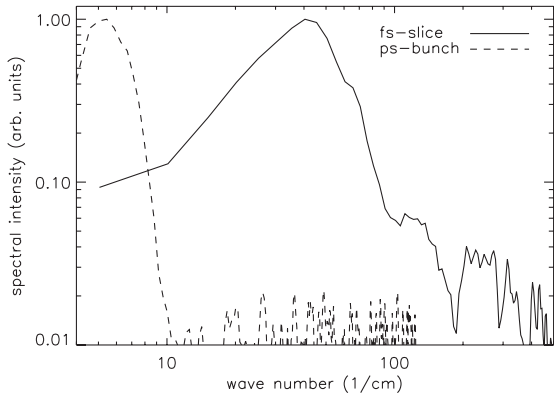

FIG. 6. THz spectra normalized to their maximum from a Gaussian bunch of 1.2 ps (rms) length and from the longitudinal density modulation induced by fs laser pulses. The integrals of both spectra correspond to THz pulse energies of nJ.

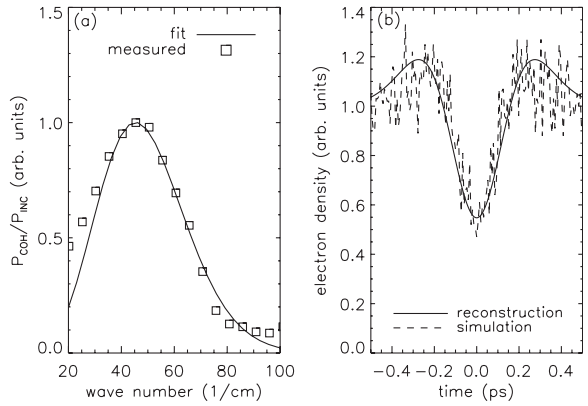

FIG. 7. Pulse shape reconstructed by an iterative method (a) in the frequency domain with measured spectral data and (b) in the time domain with data obtained by simulating electrons interacting with a fs laser pulse and their propagation through the magnetic lattice.

tribution of energy-modulated electrons and the shorter width σ_2 represents the depleted zone in the electron distribution. Under the condition $\rho(z) = 1 + G_1(z, \sigma_1) - G_2(z, \sigma_2)$ for the electron density and $\int_{\infty}^{-\infty} G_1 dz = \int_{\infty}^{-\infty} G_2 dz$, the two Gaussians were iteratively varied to fit the measured power spectrum, yielding $\sigma_1 = (210 \pm 10)$ fs and $\sigma_2 = (130 \pm 10)$ fs. The resulting pulse shape shown in Fig. 7 matches the longitudinal density distribution derived from the tracking calculations depicted in Fig. 1. The low-frequency depletion in the spectrum of laser-induced radiation in Fig. 6 is caused by destructive interference of wave trains emitted by the density maxima at ± 300 fs in the time-domain modulation in Fig. 7.

In conclusion, the measurements demonstrate the broadband emission characteristics and the fs duration of THz radiation pulses induced by femtoslicing. Their pulse energy is sufficiently high for spectroscopic experiments and comparable to broadband laser-based THz sources. In addition, THz pulses from femtoslicing are naturally synchronized to fs x-ray pulses. Besides being crucial for setting up and optimizing femtoslicing experiments, the laser-induced THz radiation itself is a useful source for time-resolved experiments.

We are indebted to the cooperation of H. J. Bäcker, J. Bahrdt, V. Dürr, J. Feikes, H.-W. Hübers, W. B. Peatman, D. Ponwitz, U. Schade, G. Wüstefeld, and others. The work is supported by the Bundesministerium für Bildung, Wissenschaft, Forschung und Technologie and by the Land Berlin.

*Electronic address: holldack@bessy.de

[1] In SASE FEL at the TESLA Test Facility, Phase 2, Technical Design report, Deutsches Elektronen Synchrotron, DESY, Report No. TESLA-FEL 2002-1, Hamburg (2002).
[2] B. Ferguson and X.-C. Zhang, Nat. Mater. **1**, 26 (2002).
[3] A. A. Zholents and M. S. Zolotorev, Phys. Rev. Lett. **76**, 912 (1996).
[4] R. W. Schoenlein *et al.*, Applied Physics (New York) **71**, 1 (2000).
[5] K. Holldack, S. Khan, R. Mitzner, and T. Quast, Phys. Rev. ST Accel. Beams **8**, 040704 (2005).
[6] S. Khan *et al.*, in *Proceedings of the Particle Accelerator Conference, Portland, 2003*, p. 2287, http://www.jacow.org.
[7] S. Backus *et al.*, Rev. Sci. Instrum. **69**, 1207 (1998).
[8] F. Sannibale *et al.*, *Proceedings of the European Particle Accelerator Conference, Lucerne, 2004*, p. 2448, http://www.jacow.org.
[9] K. Holldack *et al.*, *Proceedings of the European Particle Accelerator Conference, Lucerne, 2004*, p. 834, http://www.jacow.org.
[10] C. J. Hirschmugl, M. Sagurton, and G. P. Williams, Phys. Rev. A **44**, 1316 (1991).
[11] J. S. Nodvick and D. Saxon, Phys. Rev. **96**, B190 (1954).
[12] 4.2 K-InSb hot-electron bolometer (QMC Ltd., Cardiff) and a 4.2 K Si bolometer (Bruker-Optics, Leipzig).
[13] 300 K-DTGS detector (Bruker-Optics, Leipzig).
[14] A. Nahata *et al.*, Appl. Phys. Lett. **69**, 2321 (1996).
[15] K. Holldack *et al.*, *Proceedings of the Particle Accelerator Conference, Knoxville, 2005*, p. 2239, http://www.jacow.org.
[16] H. Wiedemann, *Particle Accelerator Physics I* (Springer, Berlin, 1998), p. 179.
[17] P. Kung, H. C. Lihn, H. Wiedemann, and D. Bocek, Phys. Rev. Lett. **73**, 967 (1994).
[18] D. H. Martin and E. Puplett, Infrared Phys. **10**, 105 (1970).
[19] M. Abo-Bakr, J. Feikes, K. Holldack, G. Wüstefeld, and H.-W. Hübers, Phys. Rev. Lett. **88**, 254801 (2002).